ISBN: 978-3-95450-233-2 ISSN: 2673-5504 doi:10.18429/JACoW-SRF2021-MOPFDV003

MEASURING FLUX TRAPPING USING FLAT SAMPLES

F. Kramer*, S. Keckert, J. Knobloch[1], O.Kugeler, Helmholtz Zentrum Berlin, Berlin, Germany
[1]also at Universität Siegen, Siegen, Germany

Abstract

With modern superconducting cavities flux trapping is a limiting factor for the achievable quality factor. Flux trapping is influenced by various parameters such as geometry, material, and cooldown dynamics. At SRF2019 we presented data showing the magnetic field surrounding a cavity. We now present supplemental simulations for this data focusing on geometric effects. As these simulations are inconclusive, we have designed a new setup to measure trapped flux in superconducting samples which is presented as well. The advantages compared to a cavity test are the simpler sample geometry, and quicker sample production, as well as shorter measurement times. With this setup we hope to identify fundamental mechanisms of flux trapping, including geometry effects, different materials, and different treatments. First results are presented along with the setup itself.

INTRODUCTION

In superconducting cavities operating in the radio frequency (RF) range, losses occur. As the cavities are operated at a temperature around 2 K, 1 W of dissipated power in the cavities requires close to 1 kW of wall plug power to keep the temperature stable. Therefore, it is critical to reduce losses in the cavities, especially when accelerators are operated in continuous wave (CW) mode. The losses stem from the non-vanishing surface resistance of superconductors in RF fields. Part of this surface resistance is caused by trapped magnetic flux and since it is impossible to completely shield the earth's or other stray magnetic fields it is necessary to understand the fundamental flux trapping mechanism to increase cavity performance further.

In this paper we will first compare measured magnetic field surrounding a superconducting cavity with two simulations to investigate whether all components of magnetic flux are trapped or only the component perpendicular to the cavity's surface. In the simulations only a simple static model was assumed and the analysis showed that with the data set at hand no definite statement can be made.

To better understand the flux trapping mechanism we designed a new experiment that is presented in this paper. The new setup is intended to increase the accuracy of the magnetic field data as well as decrease the geometric complexity of the superconductor. The sample is a (100 x 60 x 3) mm Niobium sheet. The magnetic field ist measured by 45 anisotropic magnetoresistive (AMR) sensors mounted on a custom printed circuit board (PCB) just above the sample. Additionally the temperature can be controlled with heaters at either end of the sample. We hope that the small distance of the sensors to the sample, the high density of sensors and the simple geometry helps to overcome the problems we faced with the measurements conducted with the cavity. In addition to the setup we present data from commissioning.

* f.kramer@helmholtz-berlin.de

FLUX TRAPPING MEASUREMENTS WITH CAVITIES

In this section we analyse data showing the magnetic field surrounding a superconducting cavity already presented SRF 2019 [1]. However, since then we performed more detailed simulations with which we want to investigate how the magnetic field gets trapped inside the cavity: In particular the question whether all components of magnetic flux are trapped within the superconductor or only components perpendicular to the surface are trapped. The analysis reveals that neither of the two static models that were assumed in the simulations can describe the measured data with high accuracy. We, therefore, conclude that with the data set at hand it is not possible to make a definite statement of how the flux is trapped.

Experimental Setup

Here we only give a brief overview of the setup. A more detailed description can be found in [2]. A schematic view is shown in Fig. 1 Measurements are conducted on a 1.3 GHz

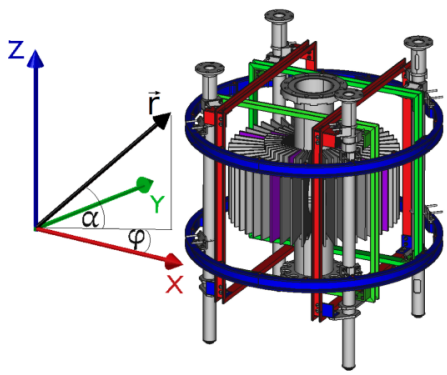

Figure 1: CAD rendering of the measurement setup consisting of a cavity in the middle, circuit boards measuring the temperature and B-field around it, and three Helmholtz coils. The blue, red, and green coils generate a field in z, x, and y directions respectively. Boards for measuring the magnetic field are highlighted purple.

TESLA single cell cavity. 48 PCBs are spaced evenly around the cavity, four of which are used to measure magnetic field. The remaining 44 are used to measure the surface temperature of the cavity. The four magnetic field mapping cards are highlighted purple, and are spaced 90° apart. On each board 15 single-axis AMR sensors are installed, forming five

ISBN: 978-3-95450-233-2 ISSN: 2673-5504 doi:10.18429/JACoW-SRF2021-MOPFDV003

sensor groups, each measuring the full 3D magnetic field vector. Additionally 3 Helmholtz coils are placed around the cavity allowing us to apply a magnetic field in an arbitrary direction.

Compare Measurements with Simulations

Two distinct models are investigated. In the first all magnetic flux is trapped. In the second model only the field component perpendicular to the cavity's surface is trapped. To distinguish between the two models we simulate the final state magnetisation. A more detailed analysis can be found in [3].

The dynamics of partial flux expulsion are difficult to model. Simulating the distribution and orientation of trapped flux in the superconductor under different hypotheses of how the trapping takes place, and by comparing the results to the measured data, we hope to gain insight into the true nature of the trapping mechanism. In particular, we study whether a simplified static model is able to provide quantitatively accurate results.

COMSOL [4] is used as a simulation tool. Rather than attempting to simulate the trapping mechanism we look at two different final magnetisation states. In the first model magnetic flux is trapped "as is", meaning all components are trapped, independent of the orientation of the magnetic field with respect to the cavity's surface. In the second model, we assume that only the component perpendicular to the cavity's surface is trapped, the field components parallel to the surface are set to zero.

In the simulations presented here, the field is applied vertically, i.e. in the direction of the beam axis. With each configuration we can then calculate the field distribution around the cavity using COMSOL, and compare the results to the measured distribution to discern the true behaviour of flux trapping. The relative permeability μ_r of the cavity material is set to 0.0001, so that it represents the cavity in its superconducting state.

Figure 2 shows a direct comparison of measured data and the simulation results where homogeneous trapping is assumed. To enable a comparison of simulated and measured data, the values from the simulation are evaluated at the actual sensor positions. This accounts for the spread in sensor positions within each sensor group.

To quantitatively compare simulation results, the relative magnetic flux density with respect to the mean magnitude for each data set is calculated for each sensor position. Thus, the absolute amount of trapped flux is removed from comparison, and only relative differences in trapped flux throughout the cavity factor in. As a result, the quotients for homogeneous flux trapping differ from the ones where non-homogeneous trapping is assumed. The results from calculating the quotients for vertically applied field are shown in Table 1.

Note that identical letters indicate sensor groups of a single card. Identical numbers indicate sensor groups at the same level. It stands out that simulation results differ for specific sensor groups. For example, we see that within both simulations sensor groups on level 1 measure a higher flux density than sensor groups on level 5. Because in the simulations flux gets trapped uniformly over the cavity, this disparity can only be explained by the fact that the sensors in sensor groups on level 4 or 5 are spread further apart within a group, and therefore, are further away from the cavity wall. Furthermore, simulated values in sensor groups on level 1

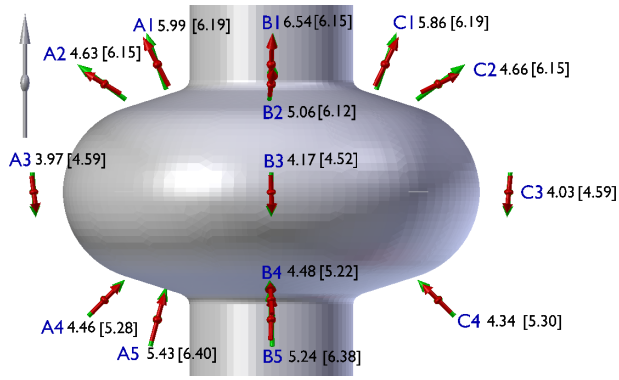

Figure 2: Measured trapped flux at the sensor positions (red) and simulation results for trapping "as is"(green). External field is applied vertically. Numbers next to the arrows show the magnitude of the measured magnetic flux density in µT. Numbers in brackets show the magnitude of the simulated magnetic flux density in µT. The grey arrow indicates the direction of the applied field, but it is not to scale. The sensor labels are marked in blue. Due to a broken sensor, sensor group C5 is not depicted.

Table 1: Magnetic flux density of measurements, simulation with homogeneous trapping, and simulation with perpendicular trapping normalized to the mean magnitude for each data set, respectively. The external field is applied vertically. If the simulation significantly (3σ = 12%) differs from the measurements, the value is highlighted in red. Due to broken sensors, sensor groups C5 and D2 are not included.

Sensor Group	Measurement	"as is" Simulation	Perpendicular Simulation
A1	1.21	1.19	1.14
A2	0.93	1.08	1.12
A3	0.80	0.83	0.84
A4	0.90	0.87	0.90
A5	1.09	1.06	1.05
B1	1.32	1.20	1.14
B2	1.02	1.09	1.12
B3	0.84	0.83	0.84
B4	0.90	0.86	0.89
B5	1.06	1.06	1.05
C1	1.18	1.20	1.14
C2	0.94	1.09	1.12
C3	0.81	0.83	0.84
C4	0.87	0.86	0.89
D1	1.35	1.19	1.14
D3	1.06	0.83	0.84
D4	0.74	0.87	0.89
D5	0.97	1.06	1.05

ISBN: 978-3-95450-233-2 ISSN: 2673-5504 doi:10.18429/JACoW-SRF2021-MOPFDV003

differ 5 to 6 percentage points across simulations, whereas, sensor groups on level 3 and 5 differ only 1 percentage point. Since the difference across simulations is larger for sensor groups on level 1 than for sensor groups on level 3 or 5, we conclude that sensor groups on level 1 are more sensitive to the hypothesis on homogeneous or perpendicular flux trapping than groups on level 3 or 5. Sensitivity differences in sensor groups on level 5 compared to sensor groups on level 1 are caused by the positioning issue mentioned above. Therefore, the sensor position should be adjusted for future experiments.

In Table 1, simulation results that differ significantly, i.e. $3\sigma = 12\%$ from the measurements are highlighted in red. The card that stands out is D, since the measurements disagree with the simulations in sensor groups D1, D3, and D4. On the other hand, sensors on cards A, B and C, agree well with simulations and with each other on levels 3-5 or 3-4 in the case of card C. On the upper half of the cavity sensors on card A, and C as well as card B, and D agree with each other. Sensors on card A and C agree with simulations on level 1 and measure less trapped flux than sensors on B, and D which agree on level 2 with simulations. So, in the upper half we see a symmetry between sensors on cards A, and C as well as on cards B, and D where each pair disagrees with simulations in one group. To summarize, we see that flux gets trapped differently in the top half than in the bottom half, and we also see that flux gets trapped differently along Card D compared to the others. We also see that for the red entries the difference between measurement and simulation is larger than the difference between the simulations.

The findings above suggest that a static model poorly reflects reality. In fact, we suspect that the dynamics of flux trapping, i.e., the changing boundary conditions as the superconducting front passes through the cavity, play an important role. Hence, using a static model to describe the entire cavity, might fall short. Therefore, inferences on the extend of flux trapping using only one or a few sensors should be treated cautiously. In such cases, only statements about the local environment are permissible. While it is a very useful tool, it should be kept in mind that the real field profile might sometimes be quite different than a static model suggests.

FLUX TRAPPING MEASUREMENTS WITH FLAT SAMPLES

Since the analysis comparing the data from the cavity measurements with simulations did not yield definite answers, a new setup is designed. With a simple sample geometry and sensors as close to the surface as possible we hope to gain insight in the mechanism of flux trapping. The simple sample geometry (100 x 60 x 3) mm also allows us to measure trapped flux for many different treatments.

Experimental Infrastructure

The experiment is conducted in a small glas cryostat depicted in Fig. 3. It is filled with liquid helium from a Dewar.

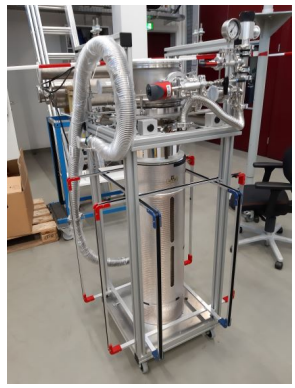

Figure 3: Picture of glass cryostat with two Helmholtz coils producing horizontal magnetic fields and a solenoid wound around the aluminium housing producing field in vertical direction.

Since the cryostat is not shielded, the earth's magnetic field has to be actively compensated. It is, therefore, necessary to be able to apply a magnetic field in an arbitrary direction. This field can then also be used to apply external field during the measurements. To achieve this, two square Helmholtz coils are attached to the holding frame of the cryostat. They create magnetic fields in two horizontal directions perpendicular to each other. Additionally a wire is wound around the aluminium housing of the cryostat itself, forming a solenoid. This provides a vertical magnetic field.

The Helmholtz coils are designed following the Helmholtz condition for square Helmholtz coils in [5]. Their magnetic field was then calculated using COMSOL. The simulation showed that in a cube of (20 x 20 x 20) cm in the centre of the Helmholtz coil the magnetic field varies less than 1%. The solenoid was simulated with COMSOL as well. It showed a deviation of the magnetic of 1.5% in the same area.

Diagnostics and Temperature Control

The experiment itself is shown in Fig. 4

We use two different kinds of sensors to measure the magnetic field. On one side of the sample three single-axis fluxgate sensors are mounted pointing in every direction in space. They are used as reference to calibrate the AMR sensors since they can not be calibrated in the intended way at cryogenic temperatures. The fluxgate sensors are also used to control the feedback loop adjusting the current in the coils to achieve a desired magnetic field.

Since fluxgates are large and expensive we use AMR sensors [6] mounted on a PCB to measure the magnetic field with a high spatial resolution, and close to the sample. The effect of the superconducting phase transition can, therefore, mostly be detected by the AMR Sensors. The PCB is depicted in Fig. 5

Sensors are soldered on small PCBs which are then soldered to the larger board to rotate the sensitive axis of the Sensors perpendicular to the plane of the main PCB. On the backside of the main board, sensors are rotated 90° with respect to the sensors soldered onto the front. By rotating

ISBN: 978-3-95450-233-2 ISSN: 2673-5504 doi:10.18429/JACoW-SRF2021-MOPFDV003

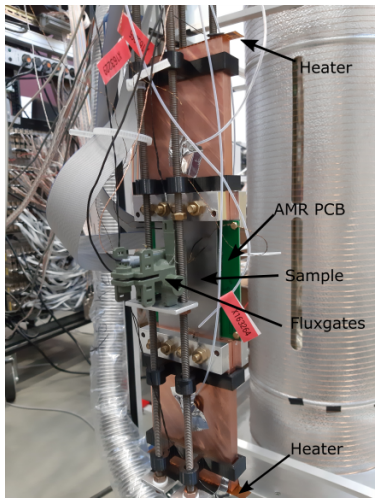

Figure 4: Picture of the assembled experiment. The niobium sample is clamped on either side with copper blocks with heaters attached at their ends. Three fluxgate sensors are mounted on one side of the sample. A PCB with AMR sensors is mounted on the other side of the sample.

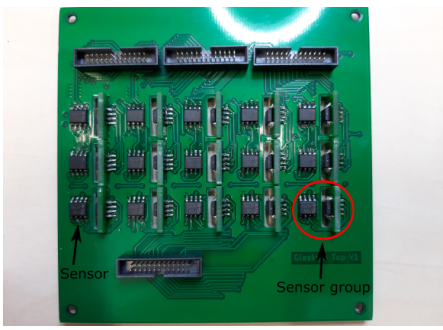

Figure 5: Picture of AMR sensors soldered to the PCB. In total 45 AMR sensors are mounted on the board. Sensors are soldered to the small adapter pieces to rotate their sensitive axis perpendicular to the plane of the PCB. On the backside, opposite to the sensors soldered directly to the board are sensors rotated 90°. By using all three types of sensors, we are sensitive in every direction. This results in a 3 x 5 grid of sensor groups.

the AMR sensors in every spatial direction we can combine three sensors in one sensor group and measure the full magnetic field vector. The dimensions of each group is (5 x 5 x 0) mm. The board is mounted at a distance of 6 mm to the sample surface. This way the sensors are more sensitive to local flux variations in the sample. A distinction between different magnetisations like in the previous chapter should, therefore, be easier. The output voltages of the AMRs are measured with an imc Spartan device [7]. With this all sensor channels are read out simultaneously with a maximum repetition rate of 500 Hz.

The sample temperature is monitored with four Cernox sensors glued to the sample. To accomplish different temperature gradients across the sample, we need to be able to control the temperature at the ends of the sample independently. For this purpose 5 mm of the sample is clamped in a copper block at either end (Fig. 4). The copper blocks are heated with a foil heater at their far side. The purpose of the long blocks is to move the electrical heater away from the sample. This reduces the magnetic field created by the heater currents at the sample. The heater power is controlled by a PID controller using the the Cernox sensors at the ends of the sample as input variable.

Measurement Procedure

The cryostat is filled with liquid helium just below the experiment. Since there is some space between the experiment and the bottom of the cryostat, we can fill roughly 2 l of liquid helium before it reaches the experiment itself. When filling the helium it evaporates and the cold gas is used to cool the experiment below transition temperature of niobium (9.2 K). However, since the the experiment is not submerged in liquid helium, we can use the heaters to heat the sample above transition temperature. When it is normal conducting, we can lower the temperature at the ends in a controlled manner with the PID controlled heaters. If there is not enough cooling power by the surrounding gas, we can evaporate some of the helium below the experiment, with an extra heater, to increase the gas flow and, therefore, cooling power. Alternatively we can evaporate helium by pumping down the pressure in the cryostat. During the cooldown a magnetic field can be applied in an arbitrary direction. When the sample is fully superconducting the ”zero-field”, i.e. the coil currents that compensated the ambient magnetic field when the sample was normal conducting, is applied again. The magnetic field measured by the AMR sensors is then just the trapped flux.

Additionally the AMR sensors need to be calibrated once the cryostat is cold, since their sensitivity is temperature dependent. For calibration the sample has to be normal conducting, so it does not influence the magnetic field. The current in each coil is successively ramped up and the output voltage of the AMR sensors measuring in the direction of the field is compared to the magnetic field measured by the corresponding fluxgate sensor. This means that inhomogeneities in the magnetic field are included in the calibration and can not be measured with the AMR sensors. The inhomogeneities can stem from an inhomogeneous ambient magnetic field, or by errors in the magnetic field created by the Helmholtz coils.

Results

In this section we will present first data acquired with the setup. The data presented here was acquired in the commissioning run. The sample is a single crystal of niobium RRR 300, which was not treated in any form.

Active Field Compensation After AMR calibration and with active compensation of the earth’s field, the fluxgates which are used as reference for the coil currents showed a magnetic field of (0.13, -0.12, 0.02) µT. The AMRs, however, show up to 4 µT. Since the AMRs are calibrated to the fluxgates, this indicates that the AMRs see field not only by

ISBN: 978-3-95450-233-2 ISSN: 2673-5504 doi:10.18429/JACoW-SRF2021-MOPFDV003

the coil it should be sensitive to, but field of the other coils as well. This can have several reasons: If the experiment is not parallel or perpendicular to the coils, the sensors will pick up a component of the field. However, in this case all sensors should pick up the same amount. We saw that some sensors measured an increase in magnetic field and some a decrease. This indicates that the sensors are not soldered perfectly to the board. We calculated the angle the sensors have to be wrong in order to see these errors is just 3°, making this explanation reasonable.

In forthcoming runs the calibration routine will be altered and the angle of the sensors will be calculated from the response to the different coils.

Temperature Control The heaters on top and bottom of the copper block allow us to create temperature gradients across the sample. In the commissioning run we achieved temperature differences between the top and bottom sensor of (0.1 - 2.5) K. Since the temperature sensors are 8 cm apart this results in a temperature gradient of (0.013 - 3.13) K/cm. Figure 6 shows the temperature of the four Cernox sensors on the sample, as well as the temperature of the surrounding gas for a cooldown with a temperature difference between top and bottom of 0.2 K (at 9.2 K).

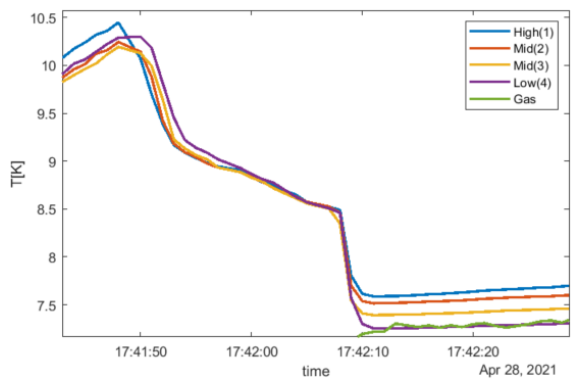

Figure 6: Temperature curve of a cooldown with a temperature difference between top and bottom of 0.2 K (at 9.2 K sample temperature)

Magnetic Field Data Figure 7 shows the measured magnetic field before and after the superconducting phase transition when the zero-field is applied. We can see in the rendering on the right in Fig. 7 that there is more trapped flux on the top of the sample. This indicates that the temperature control has to be refined to have a constant gradient across the sample.

CONCLUSION

The measurements on the cavity left open questions as to how the trapped flux inside the cavity is distributed. There are two factors that complicate the analysis: First, the distance between sensors and the cavity's surface. Second, the complex geometry of the cavity. A new experiment is designed to remedy these factors. With the this setup we are able to investigate how flux gets trapped under different external field orientations and different temperature gradients.

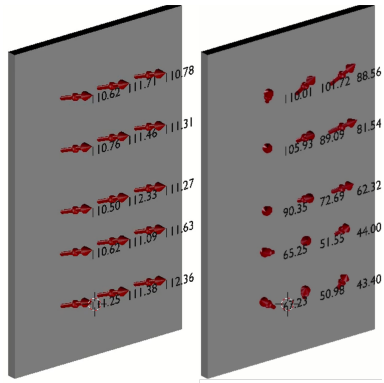

Figure 7: Magnetic field measured with AMR sensors before phase transition (left), and after phase transition when the zero field is applied (right). For this cooldown the temperature difference is 0.2 K across the sample.

Since the samples are easier and cheaper to produce than cavities, flux trapping measurements can be conducted on many different materials and treatment options. For a upcoming test the effect of a grain boundary between two large crystals is planned to be investigated.

REFERENCES

[1] F. Kramer, J. Knobloch, O. Kugeler, and J.M. Köszegi, "Mapping Flux Trapping in SRF Cavities to Analyze the Impact of Geometry", in *Proc. SRF'19*, Dresden, Germany, Jun.-Jul. 2019, pp. 364–369. doi:10.18429/JACoW-SRF2019-TUFUB3

[2] B. Schmitz, J. Köszegi, K. Alomari, O. Kugeler, and J. Knobloch, "Magnetometric mapping of superconducting RF cavities", *Rev. Sci. Instrum.*, vol. 89, p. 54706, 2018. doi:10.1063/1.5030509

[3] F. Kramer, O. Kugeler, J.-M. Köszegi, and J. Knobloch, "Impact of geometry on flux trapping and the related surface resistance in a superconducting cavity", *Phys. Rev. Accel. Beams*, vol. 23, p. 123101, 2020. doi:10.1103/PhysRevAccelBeams.23.123101

[4] COMSOL, https://www.comsol.com, 2021.

[5] A. F. R. Álvarez *et al.*, "Study and Analysis of Magnetic Field Homogeneity of Square and Circular Helmholtz Coil Pairs: A Taylor Series Approximation", in *2012 VI Andean Region International Conference*, 2012, pp. 77-80. doi:10.1109/Andescon.2012.27

[6] "Aff755b magnetoresistive field sensor", Sensitec GmbH, 2018.

[7] imc SPARTAN, https://www.imc-tm.com/products/daq-systems/imc-spartan/overview/